Magnesium Technology 2011
Edited by: Wim H. Sillekens, Sean R. Agnew, Neale R. Neelameggham, and Suveen N. Mathaudhu
TMS (The Minerals, Metals & Materials Society), 2011

Limitation of current hardening models in predicting anisotropy by twinning in hcp metals: Application to a rod-textured AM30 magnesium alloy

A. L. Oppedal[1], H. El Kadiri[1], C. N. Tomé[2], J. C. Baird[1], S. C. Vogel[2], M. F. Horstemeyer[1]

[1]Mississippi State University, Mississippi State, MS 39762, USA
[2]Los Alamos National Laboratory, Los Alamos, NM 87545, USA

Keywords: magnesium, deformation twinning, twin accommodation effects, crystal plasticity

Abstract

When a strongly textured hexagonal close packed (HCP) metal is loaded under an orientation causing profuse twinning or detwinning, the stress-strain curve is sigmoidal in shape and inflects at some threshold. Authors have largely attributed the dramatic stress increase in the lower-bound vicinity of the inflection point to a combined effect of a Hall-Petch mechanism correlated to grain refinement by twinning, and twinning-induced reorientation requiring activation of hard slip modes. We experimentally and numerically demonstrate that these two mechanisms alone are unable to reproduce the stress-strain behaviors obtained under intermediate loading orientations correlated to in-between profuse twinning and nominal twinning. We argue based on adopting various mechanistic approaches in hardening model correlations from the literature. We used both a physics dislocation based model and a phenomenological Voce hardening model. The HCP material is exemplified by an extruded AM30 magnesium alloy with a $\langle 10\bar{1}0 \rangle$-fiber parallel to the extrusion direction.

Introduction

In this work, by using a $\langle 10\bar{1}1 \rangle$ fiber texture and adopting the same correlations approaches used in the literature, we derive an important discrepancy in the prediction of the stress-strain behaviors measured under loading orientations with intermediate volume fractions of twins. Only the stress-strain behaviors under orientations completely prohibiting twinning and maximizing twinning could be acceptably reproduced. In between, the models do not provide enough precision to capture the hardening trend. We demonstrate that the reason lies behind a misunderstanding of the nature of twin-slip interactions.

A first misunderstanding comes from the Hall-Petch effect. In fact, on one hand we show that the measured twin volume fraction evolution is incompatible with the evolution of the Hall-Petch effect needed to capture the increasing hardening rate in Regime II of the stress-strain behavior. The dislocation based model is more sensitive to this effect, since no good correlations could even be achieved for the two classical limiting loading orientations. In fact, in contrast to Zr, the curves from profuse twinning and nominal twinning do not saturate at the same level in Mg, and this could not be captured by any simulation with Hall-Petch terms. On the other hand, the Hall-Petch effect accounted for by a sort of slip-twin latent hardening in the Voce type hardening model was not able to inflect the simulated curves with loading at an obtuse angle from ED.

A second misunderstanding comes from disregarding the dislocation transmutation effects upon twin incorporation [1]. The Voce model is unable to capture this effect, but the dislocation model [2] is. A pragmatic factor distinctly increasing the stored dislocations in the twin over that of the parent had an encouraging effect on modeling anisotropy in HCP metals using the transmutation effects.

We use an extruded, rod-textured, AM30 magnesium alloy obtained by relatively fast extrusion with high ratio at high temperature. Neutron diffraction, x-ray diffraction (XRD) and electron backscatter diffraction (EBSD) analyses were used to measure the deformation texture and evolution of volume fractions of twins. The VPSC code is used for the polycrystalline plasticity simulations with the dislocation-based model and an extended Voce hardening model.

Materials and Testing

The material is an AM30 Magnesium alloy received from Timminco in the form of a 200 mm diameter billet extruded from a 450 mm diameter as-cast ingot. The extrusion operated at 570 °C and at a 0.3 m/s extrusion speed.

Samples were prepared for testing along four different loading paths (Figure 1). Conventionally, previous investigators chose loading paths to maximize and minimize the effect of twinning on the mechanical be-

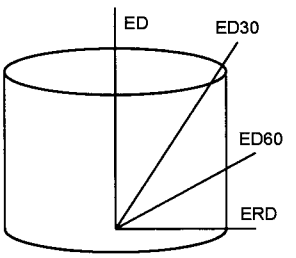

Figure 1: Schematic of sample orientations.

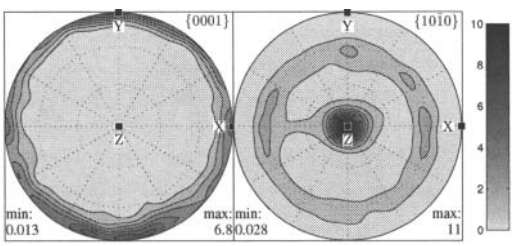

Figure 2: {0001} and {10$\bar{1}$0} pole figures obtained by neutron diffraction on an untested specimen. Z corresponds to extrusion direction; X and Y correspond to the extrusion tangent and extrusion radial directions, respectively. A pronounced ED $\parallel$ {10$\bar{1}$0} fiber from the extrusion process is evident.

havior. In this study, additional intermediate loading paths were desired, and were obtained by extracting samples at intermediate orientations. Samples were prepared allowing loading along the Extrusion Direction (ED), 30 degrees from the extrusion direction (ED30), 60 degrees from the extrusion direction (ED60), and perpendicular to the extrusion direction, i.e. extrusion radial direction (ERD).

The macrotexture information in this study was collected by neutron diffraction using using the facilities of LANSCE (Los Alamos Neutron Science) at Los Alamos National Laboratory. Details of the LANSCE facility can be found in papers by Von Dreele [3] and Wenk et al. [4]. Texture analyses and pole figure plots were done using popLA [5] and pole8 [6] software from Los Alamos National Laboratory, and MTEX [7].

The mechanical tests corresponded to uniaxial compression at room temperature and at a rate of 0.001 s^{-1}. The intermediate loading directions (30ED and 60ED) were performed in an effort to test the hardening models and correlation approaches used in the literature to fit the entire yield surface domain corresponding to various levels of twin activity.

The specimens all yielded at approximately 100 MPa, but the strain hardening behavior was markedly different. This difference is not monotonic upon angle deviation from ED toward ERD. The ED curve is pronouncedly inflecting as all grains twinned. The ERD shows an apparent permanent decreasing hardening rate characteristic of slip preponderance. The difference between ED and ERD is in contrast with the difference between TTC and IPC typically encountered in compression of c-axis fiber textures. In fact, for c-axis fiber textures, the TTC loading orientation, equivalent here to ERD, is harder than IPC, because of the necessity of harder slip mode to accommodate deformation along the c-axis. Here, upon ERD, basal slip is the predominant deformation mode with a nominal contribution of twinning. The deformation texture in Figure 2 substantiates twinning of grains having their c-axis around the normal to the ERD (highest Schmid factors).

The ED sample, with profuse twinning, shows a higher saturation stress over all other curves. The 30ED sample broke before a perceptible completion of the saturation behavior. However, the trend indicates an overreaching saturation higher than 60ED curve. The higher saturation stress upon twinning than upon slip was recently reported for basal textured pure magnesium Oppedal et al. [8]. The 30ED and 60ED stress-strain curves (Figures 3b and 4b) shows not a quite intermediate response between ED and ERD curves. The 60ED starts higher and tends to saturate lower than 30ED. However, ERD seems to violate this tendency including the saturation regime. The overlapping between curves from all loading orientations is a signature of a complex twin-slip interaction in this rod-textured magnesium alloy.

The polycrystal plasticity model and hardening rules

This work uses and compares two different hardening rules and twinning behaviors within the VPSC code. The VPSC code is based on the Visco-Plastic Self-Consistent model to compute stress in grains and can incorporate hardening rules and texture information to simulate the stress-strain behavior and deformation texture evolution together with twinning. The code models polycrystalline aggregates using single crystal constitutive rules. The VPSC scheme, developed by Molinari et al. [9] and implemented by Lebensohn and Tomé [10], estimates the stress, σ, via micromechanics applied to crystals. The hardening response is based on updating the critical resolved shear stress τ^a following the constitutive power law that provides the shear strain rate $\dot{\gamma}^a$ in each slip mode α based

on the Schmid factor m^α and a constant $\dot{\gamma}_0$ reflecting the macroscopic strain rate:

$$\dot{\gamma}^\alpha = \dot{\gamma}_0 \left| \frac{m^\alpha \overline{\overline{\otimes}} \sigma}{\tau^\alpha} \right|^n \text{sign}\left(m^\alpha \overline{\overline{\otimes}} \sigma\right) \quad (1)$$

The first hardening rule used in our simulations is the extended Voce model, described in the original work by Lebensohn and Tomé [10]. Agnew et al. [11] used the model in describing the behavior of Magnesium. In the extended Voce model, hardening in individual grains is described by:

$$\hat{\tau}_s = \tau_0^s + (\tau_1^s + \theta_1^s \Gamma)\left\{1 - \exp\left(-\frac{\theta_0^s}{\tau_1^s}\right)\right\} \quad (2)$$

where the evolution of the CRSS for each slip system, s, are represented by phenomenological parameters reflecting a curve fitting approach: τ_0^s, τ_1^s, θ_0^s, and θ_1^s. Γ is the accumulated shear strain in each grain.

Latent hardening effects between slip, and slip and twin systems, are incorporated by:

$$\delta\tau^s = \frac{\mathrm{d}\hat{\tau}^s}{\mathrm{d}\Gamma} \sum_{s'} h^{ss'} \delta\gamma^{s'} \quad (3)$$

where $h^{ss\prime}$ is a matrix of latent hardening parameters. Parameters for the Voce model simulations in this work are listed in Table 1.

The dislocation based model uses dislocation densities on different active modes to capture hardening. This model was fully described by Beyerlein and Tomé [2] where the authors used clock-rolled Zirconium, another HCP metal.

The hardening rule is a temperature and strain rate dependent formulation that assumes the effects of a dislocation forest, dislocation debris (or substructure), a Hall-Petch effect on slip propagation based on dislocation mean free path within the grain, and the effects of slip and Hall-Petch on twin propagation. If a denotes a slip mode having s as a slip system, and β denotes a twin mode having t as a twin system, both of these effects are given by the following:

$$\tau_c^\alpha = \tau_0^\alpha + \tau_{\text{forest}}^\alpha + \tau_{\text{sub}} + \tau_{\text{HP}}^s \quad (4)$$

$$\tau_c^t = \tau_0^\beta + \tau_{\text{HP}}^t + \tau_{\text{slip}}^\beta \quad (5)$$

The critical resolved shear stresses for the slip resistance equation take the following forms for each of the forest, debris, and Hall-Petch effects, respectively:

$$\tau_{\text{forest}}^\alpha = b^\alpha \chi \mu \sqrt{\rho^\alpha} \quad (6)$$

$$\tau_{\text{sub}}^\alpha = k_{\text{sub}} \mu b^\alpha \sqrt{\rho_{\text{sub}}} \log\left(\frac{1}{b^\alpha \sqrt{\rho_{\text{sub}}}}\right) \quad (7)$$

$$\tau_{\text{HP}}^s = \mu \text{HP}^\alpha \sqrt{\frac{b^\alpha}{d_g}} \text{ for } s \in \alpha \text{ without twins} \quad (8)$$

Here, b is the Burgers vector, χ is the dislocation interaction coefficient smaller that unity, μ is the shear modulus, and d is the spacing between twin lamellae.

Dislocation density evolution is modeled by:

$$\begin{aligned} \frac{\partial \rho^\alpha}{\partial \gamma^\alpha} &= \frac{\partial \rho_{\text{generation}}}{\partial \gamma^\alpha} - \frac{\partial \rho_{\text{removal}}}{\partial \gamma^\alpha} \\ &= \text{TSF} k_1^\alpha \sqrt{\rho^\alpha} - k_2^\alpha(\dot{\varepsilon}, T)\rho^\alpha \end{aligned} \quad (9)$$

The parameter k_1^α accounts for the dislocation generation, and the strain rate and temperature dependent $k_2^\alpha(\dot{\varepsilon}, T)$ accounts for dislocation removal. The TSF, or Twin Storage Factor, is a parameter first described by Capolungo et al. [12] for correlations to single crystal Magnesium work by Kelley and Hosford [13]. Oppedal et al. [8] performed experiments and numerical simulations using polycrystalline pure magnesium, providing evidence that a dislocation transmutation scheme described in El Kadiri and Oppedal [1] was responsible for the rapid strain hardening observed in HCP metals loaded to induce profuse twinning.

$$\frac{k_2^\alpha(\dot{\varepsilon}, T)}{k_1^\alpha} = \frac{\chi b^\alpha}{g^\alpha}\left(1 - \frac{kT}{D^\alpha (b^\alpha)^3} \log\left(\frac{\dot{\varepsilon}}{\dot{\varepsilon}_0}\right)\right) \quad (10)$$

Here D is termed as the drag stress, and g is the activation energy in an Arrhenius type rule for the strain rate dependence. The two critical resolved shear stresses for resistance to twin propagation relate to the Hall-Petch effect and slip and take the following forms, respectively:

$$\tau_{HP}^t = \frac{HP^\beta}{\sqrt{d_g}} \text{ with no twins or when } t \in \beta$$
$$\text{and } t \text{ is the predominant twin system (PTS)} \quad (11)$$

$$\tau_{\text{HP}}^t = \frac{HP^{\beta\beta'}}{\sqrt{d_{\text{mfp}}^s}} \text{ when } t \in \beta$$
$$\text{and } t \text{ is not the PTS, with PTS } \in \beta' \quad (12)$$

$$\tau_{\text{slip}}^\beta = \mu \sum_\alpha C^{\beta\alpha} b^\beta b^\alpha \rho^\alpha \quad (13)$$

In these equations, the Hall Petch (HP) terms are used to simulate the hardening response caused by

grain segmentation as the twin grows. However, the experimental evidence for this Hall Petch type effect, especially for twin boundaries is not substantiated. In theses simulations, the HP terms are set to zero.

In addition slip could affect twinning through the following equation:

$$\tau_{\text{slip}}^{\beta} = \mu \sum_{\alpha} C^{\beta\alpha} b^{\beta} b^{\alpha} \rho^{\alpha} \qquad (14)$$

The $C^{\beta\alpha}$ term represents the interaction between twin and slip and may be negative or positive depending on whether slip interferes with or contributes to twin growth. In simulation work presented here, we did not consider these two barriers for twin propagation for reasons that will be developed further in this paper.

The dislocation based model parameters with best fits are listed in Table 2.

Results of Simulations

In general, the several parameters in each hardening model were fit to the experimental stress-strain behavior of the ED (extrusion direction) and ERD (extrusion radial direction). The fit to the 30ED and 60ED experimental data, and comparison of the strain-hardening rate vs. stress plots were only compared after the initial fitting. Additionally, comparison of the predicted texture and experimentally measured texture at several intermediate strain levels was performed and in good agreement. Results of the texture comparison are not presented in this paper but can be found in [14].

The initial simulated values of CRSS are in agreement with those found in the literature for wrought magnesium alloys. In fact, our simulated initial strengths for basal: prismatic: pyramidal: tensile twinning were 23: 95: 111: 67 MPa, or as ratios to the easy basal slip, 1: 4.1: 4.8: 2.9. Agnew et al. [11] investigating an AZ31 alloy with c-axis fiber found initial strength ratios reported to the basal slip of pyramidal and tensile twinning to be 3 and 0.5. Proust et al. [15] investigating AZ31B and using a "composite grain" variant of the twin model reported values of ratios corresponding to prismatic: pyramidal: tensile twin to be 2.9: 5.2: 2.65.

The fit with the Voce hardening rule to the ED and ERD behaviors is satisfactory. The initial yields for the four loading orientations were all satisfactorily predicted. The hardening rate and overall response were satisfactorily captured for both ED and ERD. However, 30ED and 60ED behaviors were substantially mispredicted. 30ED prediction was the furthest from the test data since the simulated hardening rate in Regime II was of opposite sign to the measured one. It is clear that the current formulation of the Voce model does not incorporate yet a realistic understanding of twin-slip interaction. In fact, an only variation of the Schmid Factor for active deformation modes was sufficient to cause a substantial discrepancy in the prediction of anisotropy. This is atypical to the nature of the crystal plasticity framework. Therefore, it is imprudent to correlate hardening models based only on the two limiting cases of twinning contribution to deformation; intermediate contributions have to be tested as well.

Oppedal et al. [8] used the dislocation based rule to model the behavior of pure Magnesium with c-axis fiber. The corresponding initial slip resistances were found to be scalable to the ones simulated for AM30 in this study, although with a $\langle 10\bar{1}0 \rangle \parallel$ ED fiber. For each of basal, prismatic, and pyramidal modes, the values producing good correlations for AM30 were 23: 95: 111 MPa (or 1: 4.1: 4.8) compared to 11: 30: 50 MPa (or 1: 3: 4.5) for pure Magnesium. For tensile and compression twins in AM30, τ_{crit} and τ_{prop} were 67 and 25 MPa, and 275 and 275 MPa, respectively, compared to 15 and 10 MPa, and 185 and 185 MPa, respectively for pure Magnesium. As a ratio to basal slip, tensile twinning had a higher initial resistance in AM30 (2.91) than in pure Mg (1.4). This reflects the higher sensitivity to the alloying elements of twinning compared to slip.

In the case of the dislocation density model, reference must be made to the strain hardening rate versus stress plots. Figure 5 shows the result of varying the twin storage factor (TSF). It was not possible to correlate simultaneously ED and ERD stress strain behaviors unless a TSF of three was used. The effect of the TSF on the stress strain behavior is illustrated in Figure 5. Not only under ED was the saturation stress substantially underestimated with TSF=1, but under ERD as well. This is due to nominal tensile twinning under ERD not possible to prohibit under any other loading. This is in variance to the in the c-axis fiber where compression along the fiber completely prohibits tensile twinning.

In contrast to the Voce model, the dislocation density based model with the TSF was able to reproduce the mechanical responses under 30ED and 60ED when the fit was done based on ED and ERD behaviors. The robustness of this model is offered by the TSF strategy that hypothesized that the twin hardens more

importantly than parent. This hypothesis is of striking consistency with the progressive decrease in the severity of the hardening slope when the loading direction is progressively being deviated from ED toward ERD, i.e., with the progressive decrease of twinning contribution to the overall deformation.

Conclusions

The simulations are consistent with the idea of an increased hardening in the twin during profuse twinning caused by the dislocation transmutation idea put forward by El Kadiri and Oppedal [1].

In the simulations using the dislocation density hardening model, it was not possible to achieve a good model correlation to the experimental data without using a twin storage factor of three. This also gave the desirable effect of correlating fairly well the strain hardening rate versus stress behavior as well. With a twin storage factor of three, the simulations could reach the proper saturation stress levels that the experimental test data showed. The simulations also predicted well the experimentally observed stress-strain and texture behavior without utilizing a Hall-Petch type effect that has been attributed to the grain refinement by twinning. Also, the Hall Petch effect for magnesium twin boundaries has been experimentally observed to be quite low [16].

The use of the VPSC simulations with the dislocation density based hardening rule allowed a coupling between slip, twinning, texture, and stress state behavior analysis that has not fully explained by the use of empirical latent hardening parameters such as used in the Voce hardening models. Furthermore, the quantification of the slip activity, twin activity, texture evolution, and hardening as a function of strain allows for macroscale internal state variable.

Acknowledgments

The authors would like to recognize the Center for Advanced Vehicular Systems (CAVS) at Mississippi State University for supporting this work. Also, the authors gratefully acknowledge funding support through the DOE Southern Regional Center for Lightweight Innovative Design award DE-FC26-06NT42755 to carry out a portion of this research work. The authors acknowledge Alan Luo (General Motors Company), and Joy Hines Forsmark and John Allison (Ford Motor Company) for their leadership and encouragement of the larger USAMP/DOE Integrated Computational Materials Engineering for Magnesium Program. Part of this work was also supported by the U.S. Army Tank Automotive Research, Development and Engineering Center (TARDEC) under Contract No. W56HZV-04-2-0003.

References

[1] H. El Kadiri, A. L. Oppedal, J. Mech. Phys. Solids 58 (2010) 613–624.

[2] I. J. Beyerlein, C. N. Tomé, Int. J. Plast. 24 (2008) 867–895.

[3] R. B. Von Dreele, J. Appl. Crystallogr. 30 (1997) 517–525.

[4] H. R. Wenk, L. Lutterotti, S. Vogel, Nucl. Instrum. Meth. A 515 (2003) 575–588.

[5] U. F. Kocks, J. S. Kallend, H. R. Wenk, A. D. Rollett, S. I. Wright, popLA Preferred Orientation Package – LA-CC-89-18, Los Alamos National Laboratory, 1995.

[6] C. N. Tomé, Program Pole (version 8b), Los Alamos National Laboratory, 2008.

[7] R. Hielscher, H. Schaeben, J. Appl. Crystallogr. 41 (2008) 1024–1037.

[8] A. L. Oppedal, H. El Kadiri, C. N. Tomé, G. C. Kaschner, S. C. Vogel, J. C. Baird, M. F. Horstemeyer, 2010. Submitted.

[9] A. Molinari, G. R. Canova, S. Ahzi, Acta Metall. 35 (1987) 2983–2994.

[10] R. A. Lebensohn, C. N. Tomé, Acta Metall. Mater. 41 (1993) 2611–2624.

[11] S. R. Agnew, M. H. Yoo, C. N. Tomé, Acta Mater. 49 (2001) 4277–4289.

[12] L. Capolungo, I. J. Beyerlein, C. N. Tomé, Scr. Mater. 60 (2009) 32–35.

[13] E. W. Kelley, W. F. Hosford, Jr., Trans. Met. Soc. AIME 242 (1968) 5–13.

[14] A. L. Oppedal, H. El Kadiri, Q. Ma, M. F. Horstemeyer, 2010. In preparation.

[15] G. Proust, C. N. Tomé, A. Jain, S. R. Agnew, Int. J. Plast. 25 (2009) 861–880.

[16] C. H. Cáceres, P. Lukáč, A. Blake, Philos. Mag. 88 (2008) 991–1003.

Table 1: Voce parameters used in simulations.

Mode	τ_0	τ_1	θ_0	θ_1	$h^{ss'}$ Prism.	$h^{ss'}$ Basal	$h^{ss'}$ Pyr.	$h^{ss'}$ T. Twin	$h^{ss'}$ C. Twin
Prismatic	95	7	462	0	1	1	1	1	0
Basal	23	51	683	0	1	1	1	1	0
Pyramidal	111	914	3661	0	1	1	1	1	0
Tensile Twin	67	0	0	0	1.4	1.4	1.4	1	0
Compression Twin	315	0	0	0	0	1	1	0	1

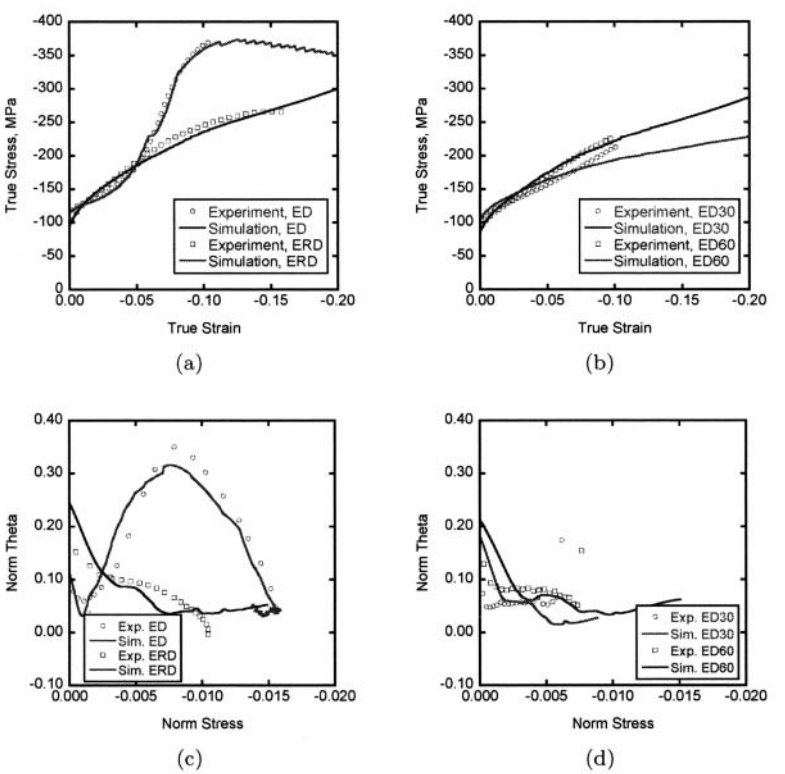

Figure 3: Comparison between experimental results and VPSC simulations using the Voce hardening rule. Stress-strain curves of the (a) extrusion (ED) and extrusion radial direction (ERD) and (b) 30 degrees (ED30) and 60 degrees (ED60) from the extrusion direction, and strain hardening rate versus stress curves for the (c) extrusion and extrusion radial direction and (d) 30 degrees and 60 degrees from the extrusion direction. In the strain hardening rate versus stress plots, stress values were normalized by $\sigma_{\text{normalized}} = (\sigma - \sigma_y)/\mu$ where σ_y is yield stress and μ is shear modulus.

Table 2: Dislocation density hardening rule parameters.

	Prism. ($\alpha = 1$)	Basal ($\alpha = 2$)	Pyr. ($\alpha = 3$)	T. Twin ($\beta = 1$)	C. Twin ($\beta = 2$)
k_1 $1/m$	1.00E+09	0.60E+09	2.00E+09		
$\dot{\epsilon}_0$ s^{-1}	1.00E+07	1.00E+07	1.00E+07		
g^α	0.0035	0.0035	0.003		
D_0^α MPa	3.40E+03	10.0E+03	0.08E+03		
τ_0^α MPa	95	23	111		
χ	0.9	0.9	0.9		
τ_{crit}^β MPa				67	275
τ_{prop}^β MPa				25	275
Twin Storage Factor				1, 3	1, 3

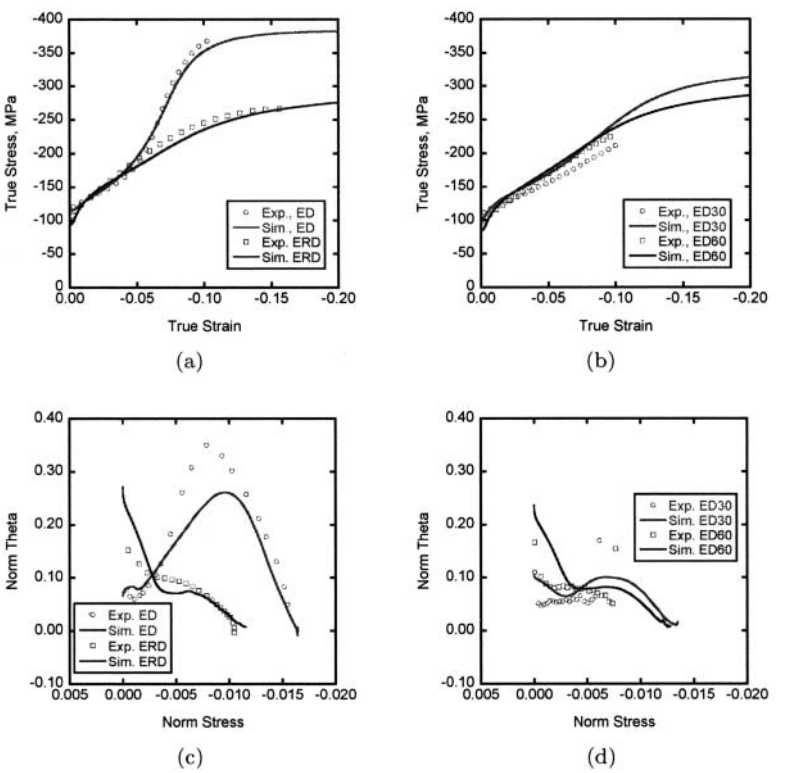

Figure 4: Comparison between experimental results and VPSC simulations using the dislocation density hardening rule. Stress-strain curves of the (a) extrusion (ED) and extrusion radial direction (ERD) and (b) 30 degrees (ED30) and 60 degrees (ED60) from the extrusion direction, and strain hardening rate versus stress curves for the (c) extrusion and extrusion radial direction and (d) 30 degrees and 60 degrees from the extrusion direction. The simulations used the parameters in Table 2 with twin storage factor equal to 3. In the strain hardening rate versus stress plots, stress values were normalized by $\sigma_{\text{normalized}} = (\sigma - \sigma_y)/\mu$ where σ_y is yield stress and μ is shear modulus.

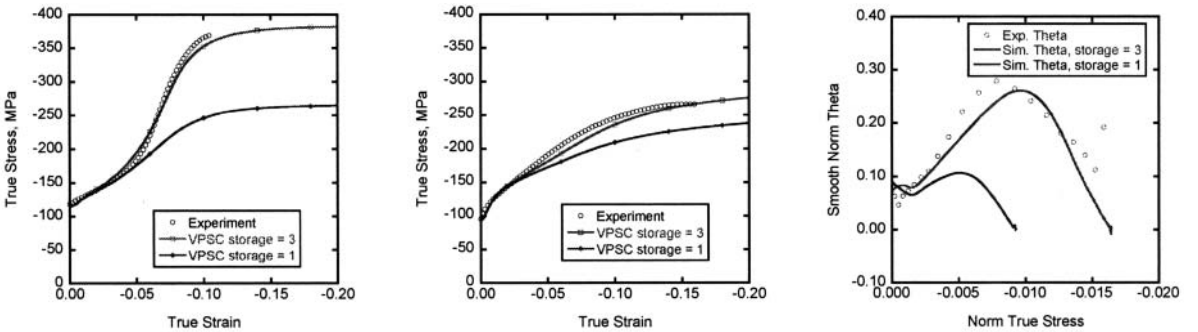

(a) ED (b) ERD

Figure 5: Results of VPSC simulations using the dislocation density hardening rule and experimental results, true stress versus true strain for two different twin storage factors. The simulation and experimental results are from uniaxial compression in a) the Extrusion Direction (ED) and b) Extrusion Radial Direction (ERD). The strain hardening rate versus stress is plotted in c), for two different values of twin storage factor.